PHYSICAL REVIEW B VOLUME 27, NUMBER 4 15 FEBRUARY 1983

Kinetics of helium self-trapping in metals

M. I. Baskes and W. D. Wilson
Theoretical Division, Sandia National Laboratories, Livermore, California 94550
(Received 3 May 1982)

A kinetic model, based upon rate theory, is presented which provides a quantitative description of the processes leading to the self-trapping of helium introduced into metal lattices either by tritium decay or by sub-damage-threshold ion implantation. The model makes use of previously published binding energies of helium, vacancies, and self-interstitials to each other. A coupled set of diffusion and rate equations allowing for the diffusion of helium interstitials, vacancies, and tritium atoms and the trapping of helium, vacancies, and self-interstitials in clusters is solved with the use of methods applicable to those stiff equations. The results are compared with the tritium decay experiments of Thomas, Swansiger, and Baskes and the low-energy implantation experiments of Thomas and Bastasz. The model provides the necessary link between these experiments and the atomistic theory.

I. INTRODUCTION

Very recently, the concept of self-trapping of helium in metals was proposed[1,2] and experimentally verified by low-energy ion implantation.[3] These atomistic calculations form the basis of a model which is capable of explaining the well-known observation that helium, however introduced into a metal lattice, will remain trapped in the lattice until thermally desorbed at very high temperatures.[4–8] In addition, the atomistic calculations are the first to verify the proposed mutation process[6] of helium-filled single vacancies into multiple vacancies.

The calculations of the trapping of helium atoms in nickel (and copper) show that the helium atoms energetically prefer to cluster rather than remain as isolated interstitials. This clustering leads to the formation of near Frenkel pairs (lattice atoms spontaneously pushed into nearby interstitial sites) which themselves cluster into self-interstitial "loops." These loops substantially increase the binding energy of the helium atom to the cluster. Binding energies of helium, vacancies, and self-interstitial atoms as a function of cluster size were obtained yielding an atomistic explanation of the fact that helium, even in low concentrations, remains trapped in a metal lattice undergoing thermal desorption until very high temperatures are reached. Static atomistic calculations by themselves, however, do not provide the necessary kinetic description involving the competing process of migration and trapping of defects, nor do they provide the details of the growth and diminution of clusters as a function of temperature. It is this description that is provided here. This kinetic model thus provides the necessary link between the atomistic theory,[1,2] the tritium decay measurements,[8] and the low-energy implantation results.[3]

In Sec. II the model is described and the governing equations are presented. The model is applied to both tritium decay experiments and low-energy implantation experiments. These calculations are presented in Sec. III which also contains a discussion of the results. Section IV contains a summary.

II. RATE PROCESSES

A. Rate equations

In order to model ^{3}He release from solids containing tritium it is necessary to know the time and spatial variation of the tritium which produces ^{3}He in the lattice by the β^- decay process: $T \rightarrow {}^3He + \beta^- + \bar{\nu}$. The β^- particle has an average energy of 5.6 keV and an end-point energy of 18 keV, which is too low to produce lattice damage in a metal. (The antineutrino $\bar{\nu}$ is required for spin conservation but has no importance to us in this work.) The ^{3}He atom is thus "implanted" in the lattice in the absence of damage with an $\sim$1-eV recoil energy which is easily dissipated into lattice phonons or may result in a helium jump. In a one-dimensional model, the concentration of tritium in the lattice C_T is described below:

$$\frac{\partial C_T}{\partial t} = \frac{\partial}{\partial x}\left[D_T \frac{\partial C_T}{\partial x}\right] - \lambda C_T \,, \tag{1}$$

where λ is the tritium decay constant, D_T the tritium diffusion coefficient $(2.3\times10^{-3}\exp[(-0.41\ \text{eV})/kT]\ \text{cm}^2\,\text{sec}^{-1}$ for Ni) from Ref. 9, t the time, and x the spatial variable, measured from the sam-

ple surface.

The helium atoms produced from either the tritium decay (or low-energy implantation at a rate G) are allowed to diffuse interstitially with a coefficient D_{He}, and, as stated above, may cluster and spontaneously form vacancies (at a critical number of helium atoms), which the helium immediately occupies. The concentration of interstitial helium C_{He} is therefore growing via the detrapping of helium from clusters (i,j) of concentration C_{ij} (containing i vacancies and j helium atoms) and diminishing via the capture of interstitial helium by such clusters:

$$\frac{\partial C_{\mathrm{He}}}{\partial t}=\frac{\partial}{\partial x}\left[D_{\mathrm{He}}\frac{\partial C_{\mathrm{He}}}{\partial x}\right]+\lambda C_{\mathrm{T}}+G + \sum_{i=0}^{N_V}\sum_{j=0}^{N_{\mathrm{He}}}(\nu_{ij}^{\mathrm{He}}C_{ij}-\mu_{ij}^{\mathrm{He}}C_{\mathrm{He}}C_{ij}) , \quad (2)$$

where the ν_{ij}^{He} and μ_{ij}^{He} are detrapping and capture coefficients defined below, and N_V and N_{He} are the maximum numbers of vacancies and helium atoms allowed in the clusters (i,j), respectively. We emphasize that these vacancies are produced by the self-trapping process, that is, by the forces due to clustered helium and not by radiation damage.

In a similar manner, the isolated vacancy concentration C_V is changing with time according to

$$\frac{\partial C_V}{\partial t}=\frac{\partial}{\partial x}\left[D_V\frac{\partial C_V}{\partial x}\right] + \sum_{i=0}^{N_V}\sum_{j=0}^{N_V}(\nu_{ij}^{V}C_{ij}-\mu_{ij}^{V}C_V C_{ij}) , \quad (3)$$

where the first term describes the (spatially dependent) diffusion of vacancies with coefficient D_V (taken to be $10^{-3}\exp[(-1.3\text{ eV})/kT]$ for Ni with an assumed preexponential and the activation energy taken from Ref. 10). The first term inside the summation represents the increase in isolated vacancy concentration via detrapping of vacancies from the clusters and the second term describes the loss of lattice vacancies through capture by a cluster (i,j).

The clusters (i,j) in our model are not allowed to diffuse over the temperature region considered here. They can, however, grow and diminish in size by a number of processes leading to a set of equations,

$$\frac{\partial C_{ij}}{\partial t}=\sum_{i=0}^{N_V}\sum_{j=0}^{N_{\mathrm{He}}}[(\nu_{ij+1}^{\mathrm{He}}+C_{ij+1}-\nu_{ij}^{\mathrm{He}}C_{ij})+(\nu_{i+1j}^{V}C_{i+1j}-\nu_{ij}^{V}C_{ij})+(\nu_{i-1j}^{I}C_{i-1j}-\nu_{ij}^{I}C_{ij}) +(\mu_{ij-1}^{\mathrm{He}}C_{ij-1}-\mu_{ij}^{\mathrm{He}}C_{ij})C_{\mathrm{He}}+(\mu_{i-1j}^{V}C_{i-1j}-\mu_{ij}^{V}C_{ij})C_V] . \quad (4)$$

The first term describes helium detrapping from a cluster containing $j+1$ helium atoms (resulting in the formation of a cluster of j helium atoms) and also helium detrapping from a cluster containing j helium atoms (resulting in the loss of a cluster of j helium atoms). Similarly the next terms describe vacancy detrapping, self-interstitial detrapping, helium capture, and vacancy capture. Note that to avoid the additional complexity of interstitial growth, self-interstitial capture or migration is not allowed explicitly in the model, but the physical picture involves the detrapping of the "punched-out" self-interstitials and their retrapping at interstitial loops in the near vicinity of the cluster.[1]

The detrapping constants ν_{ij}^{x} used in the above equations are given by the following expressions:

$$\nu_{ij}^{\mathrm{He}}=\nu_0 j e^{-E_{ij}^{\mathrm{He}}/kT} , \quad (5)$$

$$\nu_{ij}^{V}=\nu_0 i e^{-E_{ij}^{V}/kT} , \quad (6)$$

$$\nu_{ij}^{I}=\nu_0 e^{-E_{ij}^{I}/kT} . \quad (7)$$

where ν_0 is an attempt frequency (taken to be 10^{13} sec^{-1}), k is the Boltzmann constant, T is the temperature, and the E_{ij}^{x} are the detrapping energies of a helium, vacancy, or self-interstitial from a cluster (i,j) containing i vacancies and j helium atoms.

The capture constants μ_{ij}^{x} for $x=\mathrm{He},V$ are given by

$$\mu_{ij}^{x}=D_x n_{ij}^{x}/(a_0^{x})^2 , \quad (8)$$

where a_0^{x} is the diffusion jump distance for defect x (here we use 2.5 Å) and n_{ij}^{x} is the number of trapping sites for defect x to a cluster (i,j). For simplicity, an average value of n_{ij}^{x} of 10 was employed.

These equations represent discrete atomistic processes for clusters containing a manageable number of vacancies and helium atoms ($N_V\sim 2$, $N_{\mathrm{He}}\sim 20$). Clusters are, however, allowed to grow larger by helium capture at unsaturable traps. That is, although vacancy capture and self-interstitial emission by a cluster of N_V vacancies are not allowed, helium capture by a cluster of N_{He} helium atoms is allowed by considering this defect to be an unsaturable trap for helium. Thus capture of a helium atom by this trap simply results in an increase in the average number of helium atoms per unsaturable trap. The concentration of unsaturable traps, $C_{iN_{\mathrm{He}}}$, is deter-

mined through helium capture by the discrete trap of $N_{\mathrm{He}}-1$ helium atoms. That is, each time a trap with $N_{\mathrm{He}}-1$ helium atoms captures a helium atom, an unsaturable trap is formed. The average number of helium atoms per unsaturable trap $\bar{n}_i$ is given by

$$\frac{\partial(\bar{n}_i C_{iN_{\mathrm{He}}})}{\partial t}=N_{\mathrm{He}}\frac{\partial C_{iN_{\mathrm{He}}}}{\partial t}+\mu^{\mathrm{He}}_{iN_{\mathrm{He}}}C_{iN_{\mathrm{He}}}C_{\mathrm{He}}\ , \tag{9}$$

where the first term results from the formation of new unsaturable traps and the second from helium capture by unsaturable traps.

The total number of partial differential equations (PDE) is equal to $(N_V+1)(N_{\mathrm{He}}+2)$. Three equations [Eqs. (1)–(3)] result from the diffusing species, tritium, helium, and vacancies; an additional $(N_V+1)(N_{\mathrm{He}}+1)-3$ equations result from discrete clusters [Eq. (4)]; and (N_V+1) equations are necessary to describe the unsaturable traps [Eq. (9)]. For no initial tritium, helium, or vacancies in the solid, we have

$$C_{\mathrm{T}}=C_{\mathrm{He}}=C_V=C_{ij}=0\ , \tag{10}$$

$$\bar{n}_i=N_{\mathrm{He}}\ . \tag{11}$$

The boundary conditions for the diffusing species (tritium, helium, and vacancies) at the surfaces $(x_s=0,l)$ are given by

$$C_{\mathrm{T}}(x_s,t)=S_T\sqrt{P(t)}\ , \tag{12}$$

$$C_{\mathrm{He}}(x_s,t)=0\ , \tag{13}$$

$$C_V(x_s,t)=e^{-E^f_{IV}/kT(t)}\ , \tag{14}$$

where $P(t)$ is the tritium gas pressure, S_{T} the tritium solubility $(3.7\times10^{-3}\exp[(-0.16\ \mathrm{eV}/kT]$ T/Ni for Ni from Ref. 9) at one atmosphere pressure, and E^f_{IV} the vacancy formation energy (1.6 eV for Ni from Ref. 10).

B. Method of calculation

The set of $(N_V+1)(N_{\mathrm{He}}+2)$ PDE's [Eqs. (1)–(4) and (9)] with initial conditions [Eqs. (10) and (11)] and boundary conditions [Eqs. (12)–(14)] are solved numerically using methods similar to those we have previously presented.[11,12] Briefly, the spatial dependence is discretized into N nonuniform mesh points resulting in a system of $N(N_V+1)(N_{\mathrm{He}}+2)$ ordinary differential equations. By nature of the diversity of the time constants of the myriad of processes included, this system of equations is numerically stiff. Thus it is necessary to use methods appropriate to integrating such stiff systems, e.g., the Gear method.[13] Since the system of equations is coupled in the spatial dimension only by diffusion, banded solution methods allow a simultaneous solution of the entire system of equations rather than the iterative method used previously.[11,12] An alternative Monte Carlo procedure has been used to solve a similar set of rate equations for the case of helium bubble growth from damage produced from radiation.[14] This method does not, however, allow consideration of explicit spatial dependence.

The results presented here represent solutions for up to 100 spatial mesh points, a maximum of two explicit vacancies per cluster, and a maximum of 20 explicit helium atoms per cluster, leading to a system of up to 6600 differential equations. Variation of the number of mesh points, maximum vacancies per clusters, or maximum helium atoms per cluster did not lead to any significant differences in the clustering behavior reported below.

The detrapping energies E^x_{ij} used in the calculations were taken as the sum of the binding energies of our previous work[1] plus the activation energy for motion. The experimental value[15] of 0.15 eV for Ni was used for the activation energy for self-interstitial motion. It is recognized, of course, that atomistic binding energy calculations are no more accurate than a few tenths of an electron volt. Owing to the large number of binding energies, it was not possible to determine the sensitivity to each of these energies. Since the activation energy for helium motion has not been determined directly, the sensitivity of our calculations to this energy is investigated below. Furthermore, we are using this variation of the ^{3}He interstitial migration energy as a measure of the sensitivity of the calculations in a general sense.

III. APPLICATION OF THE KINETIC MODEL

A. Tritium decay

The kinetic model presented above, with calculated binding energies,[1] has been applied to the low-temperature ^{3}He desorption experiments of Thomas, Swansiger, and Baskes.[8] Because of the unexpectedly small quantities of ^{3}He released below room temperature, the early measurements of Thomas *et al.*[8] involved many changes in the experimental procedure to ensure that the release was not dominated by surface effects—that indeed the observations were of the release of ^{3}He from the sample. For our purposes, we have "approximated" the experimental conditions as follows: (1) Soak sample (125-μm Ni foil) at 500 K in 1 atm T_2 for 1200 sec; (2) cool to 100 K at 5 K/sec; (3) remove T_2 and hold at 300 K for 30 min; (4) age at 100 K for 1–5 weeks; (5) heat

to 300 K at 10 K/min.

Experimental sample-to-sample variation of these conditions can lead to different ^{3}He desorption spectra (positions of the peaks, etc.) and to differences of the order of (1—2 % in the quantity of ^{3}He retained.[8] Calculations of the effect of these variations show similar behavior. The fundamental fact we are concerned with, however, that only a few percent of the ^{3}He generated is released during the desorption step (5), is unchanged by these variations. Because ^{3}He (and ^{3}H) are mobile as interstitials in Ni at temperature of the order of 200 K or below, the complex time-temperature history of the samples (necessitated by experimental constraints) yields a nonuniform ^{3}He profile at the start of desorption [step (5)]. This profile is shown in Fig. 1 for an aging time of 5 weeks at 100 K leading to a calculated ^{3}He concentration at the sample center of 0.5 ppm. The surface is depleted of ^{3}He largely because of the diffusion of T_2 out of the sample during steps (2) and (3). In the calculation the activation energy for helium migration was taken to be 0.3 eV with a pre-exponential D_0 for 10^{-3} cm^2 sec^{-1} (this value of D_0 is used throughout this paper). It is important to note that the details of this profile near the surface depend upon the precise experimental conditions during steps (2) and (3). That is, the cooling rate and the length of time the sample is held at room temperature before aging can affect the ^{3}He profile before desorption. As stated above, this can affect the details of the ^{3}He release but not the fact that most of the ^{3}He is retained. Also shown in Fig. 1 is the calculated helium profile after desorption [step (5)]. It is readily seen that the helium released during the warm up to room temperature comes from the near-surface region (about the first 1—2 μm).

Another source of uncertainty lies in the calculations themselves, specifically in the determination of the helium interstitial activation energy. Variations of ~0.2 eV in the calculated migration energy (0.4—0.6 eV) have been reported[1,16,17] while analysis of experimental ^{3}He desorption[8] yields a migration energy of ~0.35 eV. Recent measurements indicate the ^{3}He migration energy may be as low as 0.1 eV.[18] To investigate the senstivity of the present calculations to this energy, the percentage of ^{3}He retained [based on the total ^{3}He generated at liquid-nitrogen (LN) temperatures: step (4)] during the linear ramp heating of step (5) is shown in Fig. 2 as a function of the activation energy for helium migration. The aging time used in this set of calculations was chosen so that the ^{3}He concentration at the center of the Ni foil was 0.1 ppm (1 week). In the entire range of activation energies considered here (between 0.2 and 0.50 eV), nearly total retention is found consistent with experiments.[8]

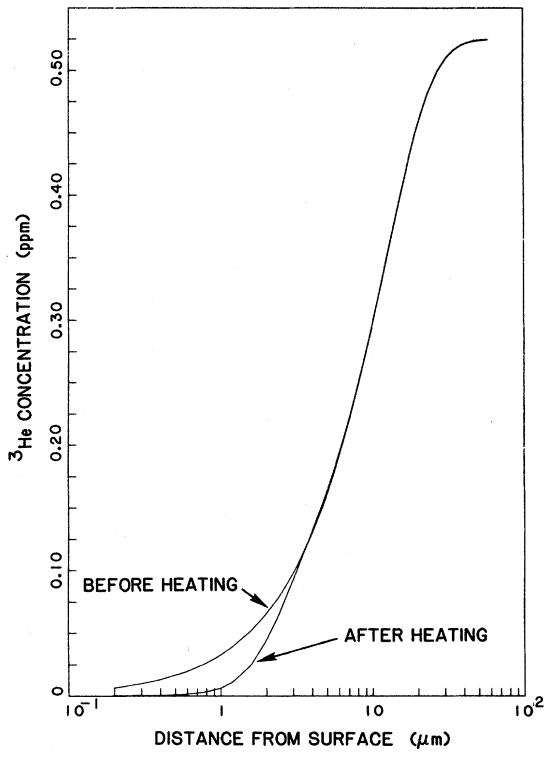

FIG. 1. Concentration of ^{3}He as a function of distance from the surface following a 5-week aging at 100 K after the standard tritium decay steps (1)—(3) in the text. The curve labeled "after heating" includes a warming stage at 10 K/min to 300 K. Note that the ^{3}He that is released upon heating comes from the near-surface region.

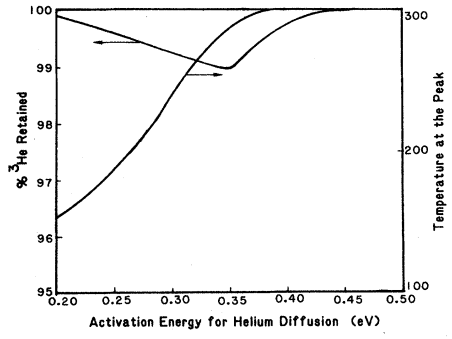

FIG. 2. Percent ^{3}He retained and temperature where the maximum release rate occurs during heating as a function of the activation energy for helium diffusion. Above an activation energy of 0.4 eV the maximum release rate occurs at 300 K where the heating is terminated.

The slight dip in the calculated release of helium as a function of activation energy may be explained as follows: When the activation energy is low (high ^{3}He-interstitial mobility), the helium can easily migrate to other helium atoms and cluster at low temperatures. This clustering, therefore, traps the helium atoms so they cannot migrate to the surface and be released. At somewhat higher activation energies, the helium mobility is reduced and clustering is delayed until higher temperatures. Some helium is, therefore, able to be released from the weakest traps [He_2 clusters are only bound by $E_B = 0.2$ eV (Ref. 1)] increasing the ^{3}He-interstitial concentration and hence the probability of release when migration temperatures are achieved. At the highest activation energies, the mobility of helium is directly reduced and the release fraction falls to zero (total retention).

Also shown in Fig. 2 is the calculated temperature at which the maximum ^{3}He desorption occurs as a function of activation energy. For activation energies above ~ 0.4 eV there is no peak, i.e., the maximum desorption rate occurs at 300 K, the highest temperature achieved upon heating. Since experiment[8] shows one or two peaks below room temperature (140–220 K), only activation energies $\lesssim 0.35$ eV are consistent with the peak location.

To illustrate the evolution of helium self-trapping, the fraction of helium atoms (relative to the amount of ^{3}He generated during the LN aging phase of the experiment) residing in the various size clusters is shown in Fig. 3 as a function of the desorption temperature achieved during the heating, step (5). The results are shown in a cumulative fashion such that the fraction of helium in a cluster (i,j) is displayed by the extent of the region labeled (i,j). For example, in Fig. 3 at 180 K, 40% of the helium is present as isolated interstitials (0,1), 20% of the helium is present as dihelium clusters (0,2), 20% as (0,3), 11% as (0,4), and the remainder as larger clusters. The calculations presented in Fig. 3 had an initial ^{3}He concentration of 0.5 ppm at the sample center. The cluster-size distribution for the 0.1-ppm case is essentially the same.

Figure 3 shows the clustering behavior at a point located at the sample center. According to the calculations, at low temperatures, essentially all of the ^{3}He exists there as isolated interstitials. As the sample is heated, first clusters of two helium atoms, and later three and more helium atoms form due to the onset of ^{3}He mobility. Between 200 and 240 K, after the isolated interstitial helium atoms have all been trapped and the temperature is still low enough to inhibit detrapping, the cluster distribution remains fixed. Above ~ 240 K, the first self-interstitial detrapping begins; that is, the cluster $He_5V^*I^*$ or (0,5)* transforms into He_5V or (1,5), by

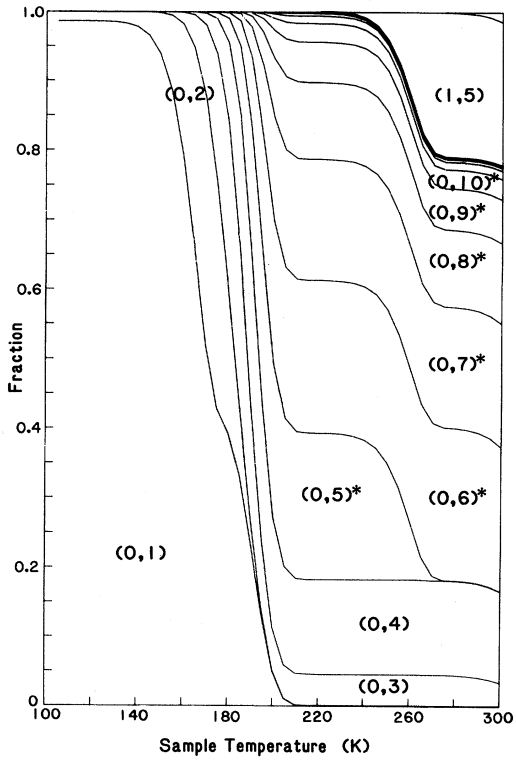

FIG. 3. Distribution ^{3}He in the various clusters as a function of sample temperature during heating for a point located at the sample center. The fraction of helium in a cluster (i,j) with i vacancies and j helium atoms is displayed by the extent of the region labeled (i,j). The clusters $(i,j)^*$ contain an unspecified numbers of near Frenkel pairs.

releasing the self-interstitial component of the near Frenkel pair.[19] By the time room temperature is reached in the desorption process, $\sim 25\%$ of the helium generated at the sample center during the aging phase is contained in clusters associated with this type of defect. The helium associated with a He_5V cluster is very deeply trapped (~ 1.35 eV).[1,2]

Figure 4 shows the different behavior which occurs near the sample surface. Here, at a depth of ~ 1 μm, the ^{3}He again starts out as isolated interstitial at LN temperature. Beginning at ~ 160 K, when the ^{3}He first becomes mobile, clusters of two helium atoms form. However, due to the lower ^{3}He concentration (see Fig. 1) near the surface (that is, a lower cross section for ^{3}He capture) combined with the close proximity to the surface (fewer number of jumps necessary to reach the surface), a large fraction of the helium reaches the surface rather than becoming trapped in larger clusters. The growth of the $H_5V^*I^*$ or (0,5)* clusters [to $He_6V^*I^*$ or (0,6)*] by helium capture (220–240 K) results in a very

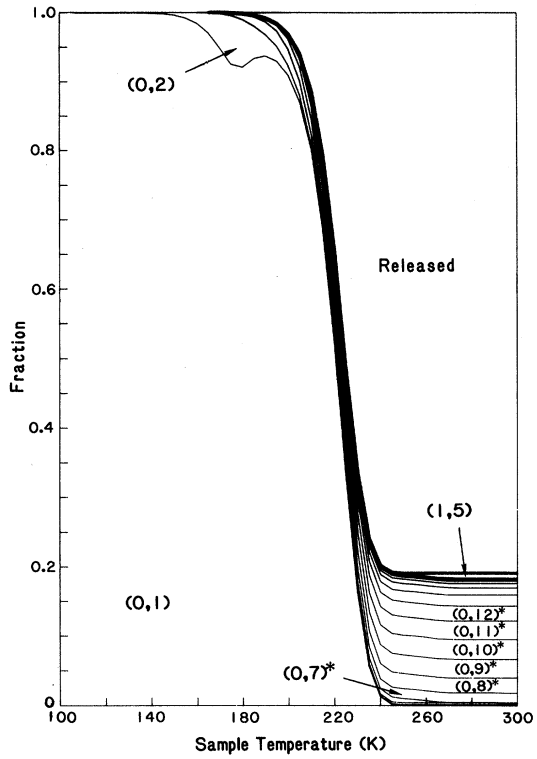

FIG. 4. Distribution in ^{3}He in the various clusters as a function of sample temperature during heating for a point located near the surface ($\sim$1-μm depth). The fraction of helium in a cluster (i,j) with i vacancies and j helium atoms is displayed by the extent of the region labeled (i,j). The clusters (i,j)* contain an unspecified number of near Frenkel pairs.

small concentration of (0,5)* clusters by 240 K. Thus, the self-interstitial emission seen in Fig. 3 is not nearly as prevalent as in the bulk (Fig. 4). As discussed above for the case of trapping at the sample center, at temperatures above $\sim$240 K when the isolated helium interstitials have all been either released or trapped, the cluster distribution stabilizes. Note that about 80% of the helium initially present at this mean-surface depth is released by room temperature (still $\lesssim$1% of the total ^{3}He) and, as above, essentially all of the remaining ^{3}He exists as small (7–15 helium atoms) clusters.

We may summarize our calculations of the tritium decay experiments as follows: (1) In agreement with experiment only a few percent of the helium generated at low temperatures is released upon heating to room temperature, (2) this helium is deeply trapped in small clusters formed by the self-trapping process, and (3) these results are insensitive to the parameter variations we have tried.

B. Low-energy implantation

As a second example of the applicability of this kinetic model, we have considered the low-energy ^{4}He implantation experiments of Thomas and Bastasz.[3] Briefly, their experiments involve implantation of thin gold foils with 300 eV ^{4}He at both 100 and 300 K with subsequent observation (at 300 K) of the foils using transmission electron microscopy. The helium atoms have insufficient energy to produce radiation damage in the gold foil. Even so, the low-temperature implantation resulted in $\sim$10-Å cavities at a density of 4×10^{18} cm^{-2} plus a higher density of larger interstitial loops in the absence of radiation damage. The room-temperature implantation, on the other hand, resulted in no apparent helium retention, and no observable features in the micrographs.

These experiments[3] were performed in gold while our helium self-trapping calculations[1,2] were performed for nickel. In our kinetics model, therefore, we chose to use the helium self-trapping energetics for nickel combined with the experimental conditions for gold. That this is reasonable for these two fcc materials was shown by our calculation of the binding of small helium clusters in gold (see Table I). We find the results do not differ markedly from those in nickel. The experimental conditions used as input to the model were as follows: implantation of a 1000-Å foil with 1.5×10^{12} He cm^{-2}sec^{-1} to a fluence of 1×10^{16} He cm^{-2} [using a reflection coefficient of 0.67 and the spatial distribution of 300-eV ^{4}He on Au (Ref. 20)], and then linear ramp heating at 10 K/min to 300 K.

The calculations are found to be in complete agreement with the central result of the experiments. Independent of the helium migration energy assumed (in the range 0.10–0.50 eV), essentially all of the helium is retained for the case of low-temperature implantation, but released during room-temperature implantation. The explanation is quite simple: At room temperature the helium simply diffuses out of the sample without encountering another helium atom [just as it did near the surface in the tritium decay experiments (Fig. 4)]. At low

TABLE I. Comparison of the binding energies of small helium clusters in nickel and gold. Note the similar binding of He_2 in both materials and the increase in binding with number of helium atoms.

Cluster	Binding energy (eV) Nickel	Gold
He_2 ($\rightarrow$He + He)	0.22	0.19
He_3 ($\rightarrow$$He_2$ + He)	0.64	0.46

temperatures the helium mobility is so low that the helium remains in the sample long enough to allow the concentration of helium to build to a level sufficient for self-trapping to occur upon heating.

It is interesting to examine the predicted size and density of unsaturable traps (formed by the helium self-trapping) as a function of implantation temperature. In Fig. 5 the predicted size and density of traps in a sample implanted at 100 K and warmed to 300 K, is shown as a function of helium interstitial migration energy. [We are here again using this quantity as a parameter to estimate the sensitivity of the results to (a) the fact that the experiments are done in Au and the binding energies calculated for Ni, and (b) there are uncertainties in experimental quantities such as the implantation temperature.] A bubble density of 4×10^{18} cm^{-3} and size of $\sim$75 helium atoms per bubble ($\sim$10 Å) are comparable to the cavities seen in gold.[3] The detectability limit of the microscope is in the 10-Å range and it is difficult to assign a specific number of helium atoms to a 10-Å cluster. We therefore chose to plot the calculated average density of "bubbles" having more than 50 He atoms in them and also the density of those containing 100 or more He atoms in order to indicate the range involved. The results are shown in Fig. 5 where the cross-hatched area is arbitrarily drawn between curves representing the 50 and 100 He atom visibility criteria. There is a cutoff as the He activation energy is increased because, as the mobility of interstitial helium is decreased, bubbles do not grow to large size. Note the experimentally determined density lies within the calculated result for activation energies in the (0.16—0.18)-eV range. The reader is cautioned, however, that no variation of the helium clustering energies was made and thus this number could change accordingly.

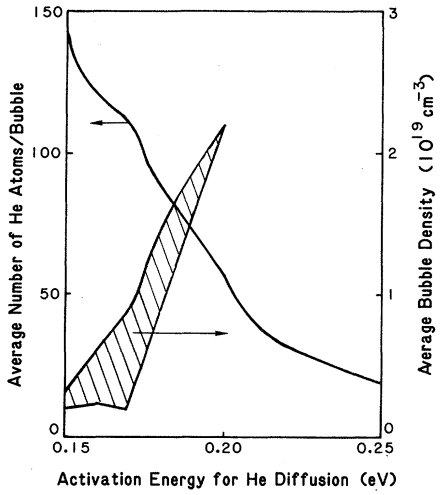

FIG. 5. Calculated bubble density and average number of helium atoms per bubble after implantation at 100 K and warming to 300 K as a function of helium activation energy for diffusion. Bubble densities of 4×10^{18} cm^{-3} have been observed in gold.

Also in Fig. 5, our calculated average number of helium atoms in a cluster is given. Clearly, since the helium is implanted in a near-surface layer nonuniformly, this bubble size (as well as the density discussed above) varies as a function of depth. We show in Fig. 5 the maximum calculated bubble size. Variation in average bubble size over the region sampled by transmission electron microscopy (TEM) ($\sim$500 Å) was less than a factor of 2. Note that as the activation energy is increased (mobility decreased) in the calculations the bubble size decreases (and the density of small bubbles correspondingly increases). Mobility enhances growth. Again, in the (0.16—0.18)-eV range, the experiment and calculation agree. The calculations also show that a large number of self-interstitials have been detrapped, resulting in the formation of dislocation loops also seen in the experiment.[3]

IV. SUMMARY

Using a set of helium and self-interstitial binding energies to clusters in Ni calculated previously, we have developed a system of coupled rate equations which take account of the complicated diffusion and trapping mechanisms occurring during a tritium decay experiment or a sub-damage-threshold implant. The details of each experiment: time-temperature sequences, soaking (in T_2) conditions, desorption rates, etc., are included in the model. Helium interstitials, vacancies, and tritium atoms are allowed to diffuse, and up to 20 helium atoms in up to two vacancies are explicitly included; the model applies only to the low temperature (at or below room temperature) regime as yet. Large clusters are treated in an unsaturable trap approximation.

The calculations provide a consistent picture of helium self-trapping as the phenomenon responsible for the nearly complex retention of helium by metal lattices up to room temperature. Calculated bubble sizes and densities are also found to be consistent with experiment. This kinetic model therefore provides the bridge between the (static) atomistic binding-energy calculations and experiment. The model is capable of describing the release behavior of helium and of providing the details of the transformation of the clusters and loops formed by the helium.

ACKNOWLEDGMENTS

The authors wish to thank L. G. Haggmark of this laboratory for communicating the results of his calculations of the range and straggling of ^{3}He in Au. This work was partially supported by the Materials Science Division of the Division of Basic Energy Sciences of the U.S. Department of Energy.

[1]W. D. Wilson, C. L. Bisson, and M. I. Baskes, Phys. Rev. B 24, 5616 (1981).

[2]C. L. Bisson and W. D. Wilson, in *Proceedings of the Conference on Tritium Technology in Fission, Fusion, and Isotopic Application, Dayton, Ohio, 1980,* compiled by L. J. Wittenberg (Southwestern Ohio Section, ANS, Miamisburg, Ohio, 1980), p. 78.

[3]G. J. Thomas and R. Bastasz, J. Appl. Phys. 52, 6426 (1981).

[4]E. V. Kornelsen, Can. J. Phys. 48, 2812 (1970).

[5]E. V. Kornelsen, Rad. Effects 13, 227 (1972).

[6]L. M. Caspers, R. H. J. Fastenau, A. van Veen, and W. F. W. M. van Heugten, Phys. Status Solidi A 46, 451 (1978); also A. van Veen and L. M. Caspers, in *Proceedings of the 7th International Vacuum Congress and 3rd International Conference on Solid Surfaces, Vienna, 1977,* edited by R. Dobrozemsky, F. Rübenauer, F. P. Viehböck, and A. Breth (R. Dobrozemsky, Vienna, 1977), p. 263.

[7]E. V. Kornelsen and A. A. van Gorkum, J. Nucl. Mater. 92, 79 (1980).

[8]G. J. Thomas, W. A. Swansiger, and M. I. Baskes, J. App. Phys. 50, 6942 (1979).

[9]W. M. Robertson, Z. Metallkund. 64, 436 (1973).

[10]W. Wycisk and M. Feller-Kniepmeier, J. Nucl. Mater. 69&70, 616 (1978).

[11]W. D. Wilson, M. I. Baskes, and C. L. Bisson, Phys. Rev. B 13, 2470 (1976).

[12]M. I. Baskes and W. D. Wilson, J. Nucl. Mater. 63, 126 (1976).

[13]C. W. Gear, *Numerical Initial Value Problems in Ordinary Differential Equations* (Prentice-Hall, Englewood Cliffs, 1971).

[14]M. I. Baskes, R. H. J. Fastenau, P. Penning, L. M. Caspers, and A. van Veen, J. Nucl. Mater. 102, 235 (1981).

[15]F. W. Young, Jr., J. Nucl. Mater. 69&70, 310 (1978).

[16]W. D. Wilson, in *Proceedings of the International Conference on Fundamental Aspects of Radiation Damage in Metals, Gatlinburg, Tennessee, 1975,* edited by M. T. Robinson and F. W. Young, Jr. (CONF-751006-P1, U.S. Energy Research and Development Administration, 1975), p. 1025.

[17]C. F. Melius, C. L. Bisson, and W. D. Wilson, Phys. Rev. B 18, 1649 (1978).

[18]D. B. Poker and J. M. Williams, private communication.

[19]Here we use the notation $(i,j)^*$ for a cluster containing i *net* vacancies (the self-interstitial component of the punched-out Frenkel pair having migrated away), with some unspecified number of near Frenkel pairs in its vicinity. As noted in Ref. 1, there is a real ambiguity as regards the definition of when a Frenkel pair has been punched out by the helium cluster. Energetically, the self-interstitial component prefers to remain in the vicinity of the cluster and how far off its normal lattice site a nickel atom should be (e.g., a half lattice constant or a first-nearest-neighbor distance) to be considered a self-interstitial is really quite arbitrary. In Ref. 1, we used the notation $He_jV_i^*I_i^*$) to represent a cluster of j helium atoms to which are attached to i near Frenkel pairs.

[20]L. G. Haggmark (private communication).